

Experimental study of weak antilocalization effects in a two-dimensional system: Anomalous dephasing rate

K. H. Gao, G. Yu,* Y. M. Zhou, W. Z. Zhou, T. Lin, J. H. Chu, and N. Dai

National Laboratory for Infrared Physics, Shanghai Institute of Technical Physics, Chinese Academy of Science, Shanghai 200083, People's Republic of China

D. G. Austing

Institute for Microstructural Sciences M50, National Research Council of Canada, Montreal Road, Ottawa, Ontario, Canada K1A 0R6

Y. Gu and Y. G. Zhang

State Key Laboratory of Functional Materials for Informatics, Shanghai Institute of Microsystem and Information Technology, Chinese Academy of Science, Shanghai 200050, People's Republic of China

(Received 9 December 2008; published 13 February 2009)

The quantum corrections to magnetoconductivity were studied in a high-mobility InGaAs/InAlAs sample with strong spin-orbit coupling. The weak antilocalization-induced drop in conductivity increases with decreasing conductivity. The experiment is well explained by theory. A spin-splitting energy larger than 5 meV obtained by fitting indicates strong spin-orbit coupling. The extracted dephasing rate as a function of temperature can be qualitatively described by modified Fermi-liquid theory with small-energy-transfer processes. Nonetheless, the extracted dephasing rate linearly increases with increasing conductivity, which is in conflict with the Fermi-liquid model.

DOI: 10.1103/PhysRevB.79.085310

PACS number(s): 73.63.Hs, 73.20.Fz, 72.20.-i

I. INTRODUCTION

The weak localization (WL) effect is caused by the constructive interference of two phase-coherent electronic waves propagating in opposite directions along the same closed trajectory.¹ This effect gives rise to a suppression of conductivity. When a magnetic field is applied perpendicular to the plane of the two-dimensional system, the constructive interference is broken as a result of a phase difference between the two electronic waves. The suppression of conductivity is gradually removed in increasing the magnetic field and consequently a positive magnetoconductivity appears. However, the WL effect is also sensitive to the spin-orbit interaction. In the presence of strong spin-orbit coupling the magnetoconductivity can change its sign, which is referred to as the weak antilocalization (WAL) effect.² The appearance of WAL effect in a two-dimensional system is thus suggestive of the presence of spin-orbit coupling. The Hamiltonian for this coupling is given by

$$H(\mathbf{k}) = \hbar \boldsymbol{\sigma} \cdot \boldsymbol{\Omega}(\mathbf{k}), \quad (1)$$

where \mathbf{k} is the electron wave vector, $\boldsymbol{\sigma}$ is the vector of Pauli matrices, and $\boldsymbol{\Omega}$ is an odd function of \mathbf{k} .

The theories of the WAL effect had been developed.³⁻⁵ The expressions from these theories are valid only for weak spin-orbit coupling in the diffusion regime. The weak spin-orbit coupling indicates that $\Omega\tau \ll 1$, where τ is the transport scattering time. In high-mobility samples, however, $\Omega\tau$ becomes comparable to unity. Therefore the experimental data cannot be successfully fitted with these theories.^{6,7} Recently, an analytical theory was developed for two-dimensional systems with strong spin-orbit coupling valid for both ballistic and diffusive regimes.^{8,9} Several experimental works done on high-mobility samples with strong spin-orbit coupling

have applied this theory. Guzenko *et al.*¹⁰ studied InGaAs/InP heterostructure using this theory and found that the obtained Rashba parameter is consistent with the values estimated from the analysis of the Shubnikov-de Haas oscillations. Spin-orbit coupling in AlGaIn/GaN heterostructures was also investigated using this model.^{11,12} Recently, our group studied a high-mobility InGaAs/InP quantum well and found that this theory satisfactorily described the experimental data over a large range of magnetic field extending from the diffusion to nondiffusion regimes.¹³ The obtained dependence of the dephasing time (τ_ϕ) on both temperature and conductivity are well accordant with existing theoretical predictions.

The electron dephasing time is an important quantity for analyzing transport in semiconductor samples since it sets the rate at which the quantum-mechanical properties of the microscopic system cross over to the classical behavior. For two-dimensional quantum well samples at low temperature, inelastic electron-electron interactions (EEIs) are the dominant dephasing process.¹ This indicates that the dephasing rate (τ_ϕ^{-1}) is proportional to the temperature (T) for the diffusive case and $\tau_\phi^{-1} \sim T^2 \ln(T)$ for the ballistic case.¹⁴ However, many experimental reports have shown results contradicting this theoretical prediction. Minkov *et al.*¹⁵ and Studenikin *et al.*⁶ observed saturation behavior of τ_ϕ at low temperature. Pagnossin *et al.*¹⁶ reported the temperature and conductivity dependences of the dephasing rate. They found that τ_ϕ^{-1} is proportional to conductivity, which contradicts the Fermi-liquid model.^{1,17} On the contrary, Eshkol *et al.*¹⁸ reported a good agreement of the temperature dependence of τ_ϕ^{-1} with modified Fermi-liquid theory¹⁴ and there was no saturation behavior of τ_ϕ at temperatures down to 130 mK. These contradictive experimental results, therefore, make it necessary to further study the dependence of the dephasing rate on temperature and on conductivity.

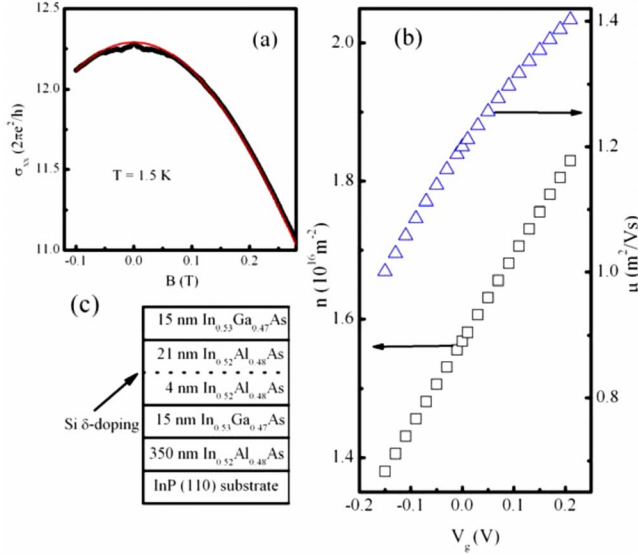


FIG. 1. (Color online) (a) Magnetoconductivity (black symbols) for $V_g = 0$ V fitted by Eq. (2). Red line is the fit. (b) Dependence of the electron density and the electron mobility on the gate voltage. Blue (black) symbols represent the electron mobility (density). (c) Schematic layer structure for our sample.

In this work, WAL magnetoconductivity was studied in a high-mobility InGaAs/InAlAs sample with strong spin-orbit coupling. We find that the experimental data can be well fitted by the recently developed theoretical model⁸ over a large range of magnetic field. The product $\Omega\tau$ and the dephasing rate are extracted. We find that $\Omega\tau$ varies from 0.98 to 1.45 and thus a large spin-split energy is deduced. The temperature dependence of the extracted τ_ϕ^{-1} can be qualitatively described by the modified Fermi-liquid theory due to small-energy-transfer processes. However, the conductivity dependence of τ_ϕ^{-1} contradicts the Fermi-liquid model.

II. EXPERIMENT

The sample used in this study is an $\text{In}_{0.52}\text{Al}_{0.48}\text{As}/\text{In}_{0.53}\text{Ga}_{0.47}\text{As}/\text{In}_{0.52}\text{Al}_{0.48}\text{As}$ quantum well grown by gas source molecular-beam epitaxy on an Fe-doped semi-insulating InP substrate. The quantum well conducting channel is formed in a 15-nm-thick layer of $\text{In}_{0.53}\text{Ga}_{0.47}\text{As}$. A single Si- δ -doped ($4 \times 10^{12} \text{ cm}^{-2}$) layer is separated from the conducting channel by a 4-nm-spacer layer. A sketch of the layer structure is shown in Fig. 1(c). After growth, the sample was processed into standard Hall bars with a front gate. The distance between the voltage probes was $400 \mu\text{m}$ and the width of the bar was $200 \mu\text{m}$. Measurements were performed in the temperature range of 1.5–8 K using standard ac lock-in techniques. The voltage (V) across the sample was varied in the range of 0.04–0.08 mV for all the gate voltages we applied to the sample. This means that $eV = 0.04\text{--}0.08 \text{ meV}$ (e is the charge of one electron), which is less than the thermal energy $k_B T = 0.13\text{--}0.69 \text{ meV}$ for the temperature range employed. This

suggests that any heating effect induced by the voltage across the sample can be neglected.

III. RESULTS AND DISCUSSION

The quantum corrections to the Drude conductivity generally have two origins: WL and EEIs. In a magnetic field the magnetoconductivity of the system can be written as

$$\sigma_{xx} = ne\mu/(1 + \mu^2 B^2) + \Delta\sigma + \Delta\sigma_{ee}, \quad (2)$$

where $\Delta\sigma$ and $\Delta\sigma_{ee}$ are, respectively, the WL and EEI corrections. $\Delta\sigma$ is dominant at low magnetic field but its influence decreases as the field increases; whereas the $\Delta\sigma_{ee}$ contribution is independent of the field. In our case, $\Delta\sigma$ includes both WL and WAL corrections because the WAL effect is also observed at very low field as seen in Fig. 1(a) for $V_g = 0$ V. From the slope of Hall resistivity, we first calculated the electron density. As shown in Fig. 1(b), the electron density linearly increases with increasing gate voltage. Neglecting $\Delta\sigma$, we fit the conductivity σ_{xx} using Eq. (2) with the obtained electron density. As seen from Fig. 1(a), Eq. (2) describes well the experimental data, which shows a parabolic trend. The mobility from the parabola fit, as seen in Fig. 1(b), increases from $1.0 \text{ m}^2/\text{Vs}$ for $V_g = -0.15$ V to $1.4 \text{ m}^2/\text{Vs}$ for $V_g = 0.2$ V. However, a noticeable deviation from this trend occurs at very small field ($|B| < 80$ mT) due to WL and WAL effects. Note that the EEI correction is included in the fit curve. The parabola is subtracted from the magnetoconductivity to extract the quantum corrections $\Delta\sigma$ originating from WL and WAL. Therefore, the quantum magnetoconductivity $\Delta\sigma$ excludes the contribution of EEI in the following analysis.

The quantum magnetoconductivity $\Delta\sigma$ at $T = 1.5$ K for several gate voltages is shown in Fig. 2. Well-developed WAL peaks are evident for all the gate voltages at $B = 0$ mT, whereas the increase of $\Delta\sigma$ for $|B| > 20$ mT can be attributed to WL that becomes dominant at larger magnetic fields. There are three characteristics in these curves to note. First, the field at which $\Delta\sigma$ shows a minimum does not depend sensitively on the gate voltage, i.e., the conductivity minimum does not change with the electron density. This means that the Rashba mechanism is the dominant spin-orbit coupling in our sample and thus the linear and cubic Dresselhaus terms in $\mathbf{\Omega}$ can be neglected in our analysis,¹⁹ which is consistent with literatures.^{20–23} Actually, the Rashba contribution to $\mathbf{\Omega}$ is expected to be large because our sample has δ doping only on one single side [see Fig. 1(c)] and so has high structure inversion asymmetry. Second, the magnetic field at which the conductivity minimum occurs is 20 mT. This value is comparable to the reported results²⁴ for an InGaAs/InAlAs quantum well sample with large spin-splitting energy (5 meV). This suggests that the spin-orbit coupling is strong in our sample because the strength of this coupling is proportional to the magnetic field at which conductivity minimum occurs.^{19,25} Moreover, from the obtained electron density and mobility shown in Fig. 1(b), we can calculate the transport magnetic field $B_{tr} = \hbar/2el^2$, where l is the transport mean-free path and \hbar is Planck's constant divided by 2π . We find that B_{tr} changes from 3.4 to 8.7 mT for all the gate voltages values

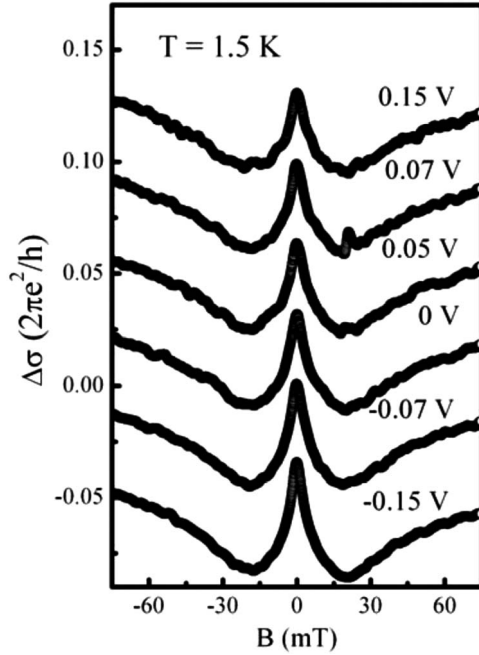


FIG. 2. The quantum magnetoconductivity $\Delta\sigma$ for several gate voltages at $T=1.5$ K. The plots are vertically shifted for clarity.

we can realize. The fact that B_{tr} is less than 20 mT at which the conductivity minimum occurs means that earlier theoretical models² cannot be used for our sample when $B > 20$ mT. In order to extract the correct value of τ_ϕ and the spin-splitting energy (ΔE_0), it is necessary to fit the magnetoconductivity for magnetic fields $B > B_{tr}$ consequently including the field at which conductivity minimum occurs in our case.¹³ The theory⁸ developed by Golub satisfies this requirement, so we use it to fit our experimental data shown below. Third, it should be noted that the WAL-induced drop in conductivity is smallest at the most positive gate voltage but becomes enhanced as the gate voltage is made more negative, i.e., the WAL-induced drop in conductivity is enhanced with decreasing conductivity, which appears contrary to the prevailing results of the WAL effect. Because the height of the WAL peak at $B=0$ T is closely related to the dephasing time, one can predict an unusual conductivity dependence of the dephasing rate.

According to Golub's theory,⁸ when the Rashba mechanism is dominant the conductivity correction due to WAL can be expressed by

$$\sigma(B) = \sigma_a(B) + \sigma_b(B), \quad (3)$$

where $\sigma_a(B)$ and $\sigma_b(B)$ can be interpreted as the respective contributions from the backscattering and nonbackscattering interference corrections to the conductivity. The detailed expressions for $\sigma_a(B)$ and $\sigma_b(B)$ can be found in Ref. 8. We used Eq. (3) to fit our experimental data. The experimental data and the fits for various gate voltages are shown in Fig. 3(a). The theory clearly describes the experimental data well up to $B/B_{tr} \sim 10$, which is higher than the field at which the conductivity minimum occurs. This enables us to accurately determine the spin-orbit coupling in our sample. The

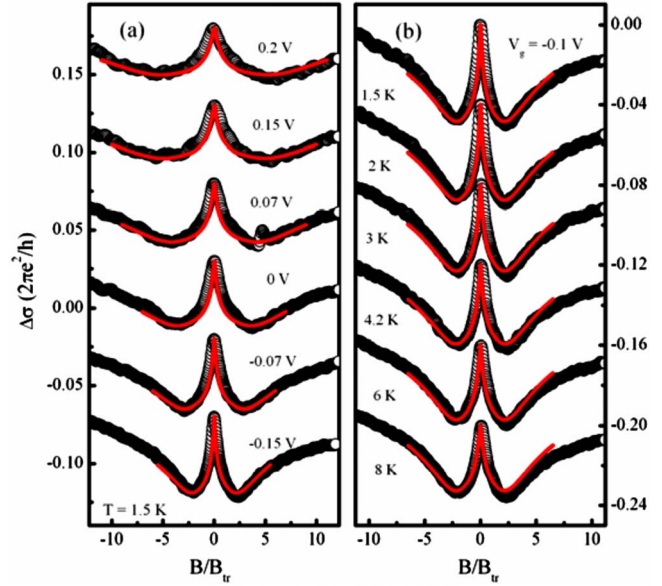


FIG. 3. (Color online) Quantum magnetoconductivity $\Delta\sigma$ (symbols) measured (a) for several gate voltages at $T=1.5$ K and (b) for $V_g=-0.1$ V at various temperatures. The curves are vertically shifted for clarity. Red lines are fits with Eq. (3).

temperature-dependent measurements shown in Fig. 3(b) for $V_g=-0.1$ V reveal a suppression of the WAL peak as the temperature increases. However, this suppression is relatively slow compared with that due to the increase in gate voltage. Again, the fitted curves follow closely the measured curves.

Figure 4(a) shows the variation in the dephasing rate τ_ϕ^{-1} with temperature extracted from the fit for $V_g=0$ and -0.1 V. According to the earlier Fermi-liquid models^{1,17,26} where only the contribution of the singlet channel interaction is considered, the dephasing rate determined by electron-electron scattering is proportional to T^2 with a large-energy-transfer mechanism but proportional to T with a small-

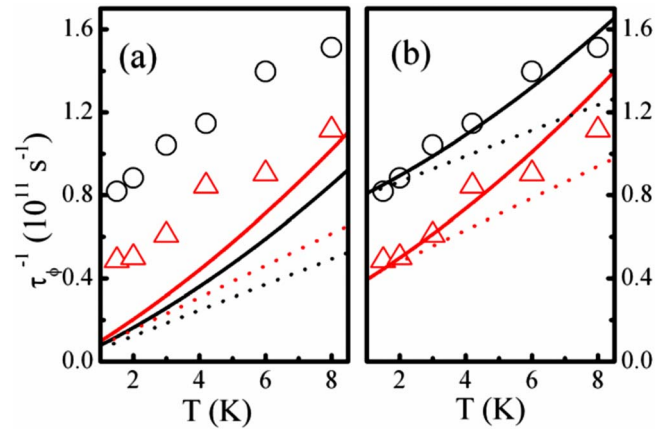


FIG. 4. (Color online) Temperature dependence of the dephasing rate τ_ϕ^{-1} extracted from fits of the weak antilocalization curves measured at $V_g=0$ (black circles) and -0.1 V (red triangles). Dotted (solid) lines are calculated with Eq. (4) [Eq. (5)]. Black and red lines are, respectively, for $V_g=0$ and -0.1 V. The calculated lines in (b) have been vertically shifted.

energy-transfer mechanism. With the mobility shown in Fig. 1(b), we calculated the parameter $k_B T \tau / \hbar$ (where k_B is the Boltzmann constant and τ is the momentum relaxation time) and found that it varies in the range 0.05–0.4, i.e., $k_B T \tau / \hbar < 1$ over the studied temperature range for all the gate voltages. This indicates that the extracted τ_ϕ^{-1} can be described by the Fermi-liquid model involving small-energy transfer,¹⁷

$$\tau_\phi^{-1} = \frac{k_B T}{\hbar} \frac{\pi G_0}{\sigma} \ln \left(\frac{\sigma}{2\pi G_0} \right), \quad (4)$$

where $G_0 = e^2 / (2\pi^2 \hbar)$. In order to compare the extracted dephasing rate with theory, we calculated τ_ϕ^{-1} using Eq. (4) [see dotted black and red lines, respectively, for $V_g = 0$ and -0.1 V in Fig. 4(a)]. The calculated curves are clearly well below the experimentally measured data points. Recently, Narozhny *et al.*¹⁴ theoretically calculated the dephasing rate including both singlet and the triplet channel interactions. Following their calculations, the temperature dependence of τ_ϕ^{-1} in the small-energy-transfer processes is

$$\tau_\phi^{-1} = \left\{ 1 + \frac{3(F_0^\sigma)^2}{(1+F_0^\sigma)(2+F_0^\sigma)} \right\} \frac{k_B T}{g\hbar} \ln[g(1+F_0^\sigma)] + \frac{\pi}{4} \left\{ 1 + \frac{3(F_0^\sigma)^2}{(1+F_0^\sigma)^2} \right\} \frac{(k_B T)^2}{\hbar E_F} \ln(E_F \tau / \hbar), \quad (5)$$

where F_0^σ is the interaction constant for the triplet channel, $g = 2\pi\hbar / e^2 R$ (R is the sheet resistance), and E_F is the Fermi energy. The solid lines shown in Fig. 4(a) are calculated from Eq. (5). Although the contribution of the triplet channel interaction is now included, the experimentally measured τ_ϕ^{-1} values are still above those calculated. This phenomenon has also been found by many groups.^{6,16,27} This discrepancy may be related to the anomalous conductivity dependence of the dephasing rate discussed below. Note that by observation if we vertically shift up the theoretical curves, we find that the theory of Narozhny *et al.*¹⁴ appears to describe better the experimental data. As seen in Fig. 4(b), we can obtain a better agreement between the theory of Narozhny *et al.* (solid lines shifted vertically) and the extracted τ_ϕ^{-1} . However, Fermi-liquid model (dotted lines shifted vertically) shows a large discrepancy with the extracted values all the same. This suggests that it is reasonable to consider the contribution of the triplet channel interaction for theory to describe the experiment. Therefore, the temperature dependence of the extracted τ_ϕ^{-1} can be qualitatively described by the modified Fermi-liquid theory¹⁴ with small-energy-transfer processes.

The inset of Fig. 5 shows the product $\Omega\tau$ as a function of gate voltage. Note that the $\Omega\tau$ increases from 0.98 at $V_g = -0.15$ V to 1.45 at $V_g = 0.2$ V, i.e., $\Omega\tau \geq 0.98$. This is indicative of very strong spin-orbit coupling in our sample. Using the relation $\Delta E_0 = 2\hbar\Omega$, the spin-splitting energy is estimated. As shown in the inset, ΔE_0 is in the range of 5.3–6.3 meV, which is comparable to the reported values of 5,²⁴ 3.82,²⁸ 5–6 (Ref. 23), and 1.6 meV (Ref. 29) for InGaAs/InAlAs quantum wells, and 1.7 (Ref. 11) and 3.8 meV (Ref. 30) for AlGaN/GaN heterostructures, and 5–11 meV (Ref. 31) for an inversion layer on InAs. This demonstrates the validity of the

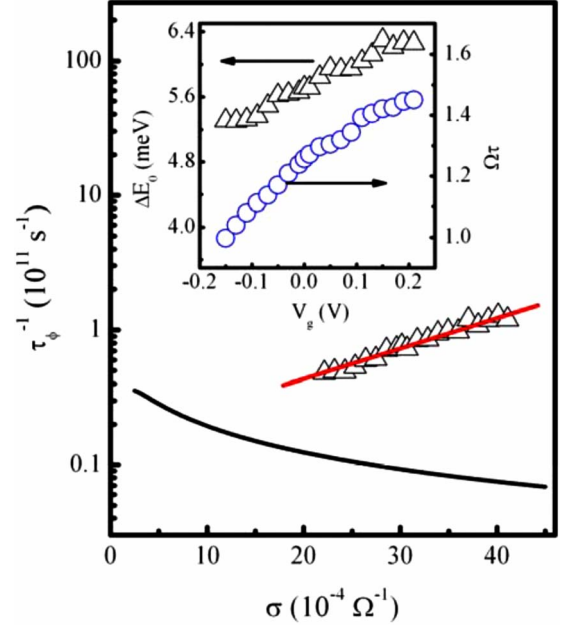


FIG. 5. (Color online) Dephasing rate τ_ϕ^{-1} versus the conductivity at $T = 1.5$ K. Black line is calculated with Eq. (4). Red line is provided as guide for the eyes. Inset shows the gate voltage dependence of the calculated spin-splitting energy at zero magnetic field and the product $\Omega\tau$ extracted by fitting the experimental data. Black (blue) symbols present the spin-splitting energy (the product $\Omega\tau$).

model⁸ for high-mobility samples with strong spin-orbit coupling. The variation of ΔE_0 with the gate voltages indicates that we can tune the spin splitting in our sample between 5.3 and 6.3 meV by varying the gate voltage between -0.15 and 0.2 V. According to the Fermi-liquid model for small-energy transfer,¹⁷ we calculated τ_ϕ^{-1} as a function of conductivity (shown as solid black line in Fig. 5). The calculated τ_ϕ^{-1} shows a monotonic decrease as the conductivity increases. The variation in the extracted dephasing rate with the conductivity is also shown in Fig. 5 for comparison (black triangles). An anomalous conductivity dependence of the dephasing rate is observed, i.e., τ_ϕ^{-1} linearly increases with increasing conductivity. This is completely contrary to the theoretical prediction. This anomalous behavior can explain the observed unusual phenomenon mentioned above, namely, the height of WAL peak at $B = 0$ T increasing with decreasing gate voltage (see Fig. 2). But, what mechanism is responsible for this anomalous conductivity dependence of the dephasing rate? Minkov *et al.*¹⁵ observed a similar phenomenon and they attribute it to the appearance of electron states at the Fermi energy in the doped layers because of the nonlinear dependence of the electron density on gate voltage in their sample. Due to the linear variation in the electron density with gate voltage in our sample [see Fig. 1(b)], we presume that there is a different mechanism for our observation. In addition to electron-electron scattering, electron-phonon interaction could plausibly affect the dephasing time and thus the dephasing rate. According to theory of the electron-phonon interaction,³² $\tau_\phi^{-1} \propto T^2/l$ for $T \gg \hbar C_l / k_B l$ and $\tau_\phi^{-1} \propto T^4 l$ for $T \ll \hbar C_l / k_B l$, where C_l is the transverse velocity of sound. Using the longitudinal-acoustic velocity³³ $C_l = 4.74$

$\times 10^3$ m/s instead of C_t , we obtain the parameter $\hbar C_l/k_B l = 0.12-0.19$ for all the gate voltages applied to our sample. Considering the relation $C_l > C_t$, we deduce that $\hbar C_l/k_B l < 0.19$. For our measurement temperature ($T=1.5-8$ K), the condition $T \gg \hbar C_l/k_B l$ is valid in our case. Therefore, the dephasing originating from the contribution of the electron-phonon scattering can be expressed as $\tau_\phi^{-1} \propto T^2/l$ (i.e., $\tau_\phi^{-1} \propto T^2/\sigma$). However, this is also in conflict with our observation (τ_ϕ^{-1} increases with increasing conductivity). Actually, the electron-phonon interaction is usually negligible at the lower end of our temperature range (1.5 K). We therefore conclude that electron-phonon scattering does not explain this anomalous behavior either. We note that recently Pagnossin *et al.* also observed this anomalous behavior of the dephasing rate both for a GaAs double quantum well¹⁶ and for two-dimensional GaAs/InGaAs heterostructures.³⁴ We hope that our observations further stimulate interest in finding the mechanism responsible for this anomalous behavior.

IV. CONCLUSIONS

In summary, weak antilocalization magnetoconductivity was studied in a high-mobility InGaAs/InAlAs quantum well

sample. The weak antilocalization-induced drop in conductivity increases with decreasing conductivity. We find that the experimental data can be well described by a recently developed theoretical model over a wide range of magnetic field. The product $\Omega\tau$ and the dephasing rate are extracted by fitting the WAL curves. We find that $\Omega\tau$ varies from 0.98 to 1.45, which together with the estimated spin-splitting energy (5.3–6.3 meV) indicates a strong spin-orbit coupling. The temperature dependence of the extracted dephasing rate can be qualitatively described by modified Fermi-liquid theory with small-energy-transfer processes. However, the conductivity dependence of the extracted dephasing rate contradicts the Fermi-liquid model.

ACKNOWLEDGMENTS

This work was supported in part by the fund of Chinese ministry of personnel, the Special Funds for Major State Basic Research under Project No. 2007CB924901, and the Science & Technology Commission of Shanghai under Grant No. 07JC14059. We thank H. Tran for the assistance with sample fabrication.

*Corresponding author; yug@mail.sitp.ac.cn

¹B. L. Altshuler and A. G. Aronov, in *Electron-electron Interactions in Disordered System*, edited by A. L. Efros and M. Pollak (Elsevier, Amsterdam, 1985).

²S. Hikami, A. I. Larkin, and Y. Nagaoka, *Prog. Theor. Phys.* **63**, 707 (1980).

³S. V. Iordanskii, Yu. B. Lyanda-Geller, and G. E. Pikus, *JETP Lett.* **60**, 199 (1994).

⁴F. G. Pikus and G. E. Pikus, *Phys. Rev. B* **51**, 16928 (1995).

⁵W. Knap, C. Skierbiszewski, A. Zduniak, E. Litwin-Staszewska, D. Bertho, F. Kobbi, J. L. Robert, G. E. Pikus, F. G. Pikus, S. V. Iordanskii, V. Mosser, K. Zekentes, and Y. B. Lyanda-Geller, *Phys. Rev. B* **53**, 3912 (1996).

⁶S. A. Studenikin, P. T. Coleridge, N. Ahmed, P. J. Poole, and A. Sachrajda, *Phys. Rev. B* **68**, 035317 (2003).

⁷S. A. Studenikin, P. T. Coleridge, G. Yu, and P. J. Poole, *Semicond. Sci. Technol.* **20**, 1103 (2005).

⁸L. E. Golub, *Phys. Rev. B* **71**, 235310 (2005).

⁹M. M. Glazov and L. E. Golub, *Semiconductors* **40**, 1209 (2006).

¹⁰V. A. Guzenko, T. Schäpers, and H. Hardtdegen, *Phys. Rev. B* **76**, 165301 (2007).

¹¹A. E. Belyaev, V. G. Raicheva, A. M. Kurakin, N. Klein, and S. A. Vitusevich, *Phys. Rev. B* **77**, 035311 (2008).

¹²W. Z. Zhou, T. Lin, L. Y. Shang, L. Sun, K. H. Gao, Y. M. Zhou, G. Yu, N. Tang, K. Han, B. Shen, S. L. Guo, Y. S. Gui, and J. H. Chu, *J. Appl. Phys.* **104**, 053703 (2008).

¹³G. Yu, N. Dai, J. H. Chu, P. J. Poole, and S. A. Studenikin, *Phys. Rev. B* **78**, 035304 (2008).

¹⁴B. N. Narozhny, G. Zala, and I. L. Aleiner, *Phys. Rev. B* **65**, 180202(R) (2002).

¹⁵G. M. Minkov, A. V. Germanenko, O. E. Rut, A. A. Sherstobitov, B. N. Zvonkov, E. A. Uskova, and A. A. Birukov, *Phys. Rev. B* **64**, 193309 (2001).

¹⁶I. R. Pagnossin, A. K. Meikap, T. E. Lamas, G. M. Gusev, and J. C. Portal, *Phys. Rev. B* **78**, 115311 (2008).

¹⁷B. L. Altshuler, A. G. Aronov, and D. E. Khmel'nitsky, *J. Phys. C* **15**, 7367 (1982).

¹⁸M. Eshkol, E. Eisenberg, M. Karpovski, and A. Palevski, *Phys. Rev. B* **73**, 115318 (2006).

¹⁹S. Schmult, M. J. Manfra, A. Punnoose, A. M. Sergent, K. W. Baldwin, and R. J. Molnar, *Phys. Rev. B* **74**, 033302 (2006).

²⁰G. Lommer, F. Malcher, and U. Rössler, *Phys. Rev. Lett.* **60**, 728 (1988).

²¹B. Das, D. C. Miller, S. Datta, R. Reifenberger, W. P. Hong, P. K. Bhattacharya, J. Singh, and M. Jaffe, *Phys. Rev. B* **39**, 1411 (1989).

²²J. Luo, H. Munekata, F. F. Fang, and P. J. Stiles, *Phys. Rev. B* **41**, 7685 (1990).

²³J. Nitta, T. Akazaki, H. Takayanagi, and T. Enoki, *Phys. Rev. Lett.* **78**, 1335 (1997).

²⁴W. Z. Zhou, T. Lin, L. Y. Shang, G. Yu, Z. M. Huang, S. L. Guo, Y. S. Gui, N. Dai, J. H. Chu, L. J. Cui, D. L. Li, H. L. Gao, and Y. P. Zeng, *Solid State Commun.* **143**, 300 (2007).

²⁵N. Thilloßen, S. Cabañas, N. Kaluza, V. A. Guzenko, H. Hardtdegen, and T. Schäpers, *Phys. Rev. B* **73**, 241311(R) (2006).

²⁶W. E. Eiler, *J. Low Temp. Phys.* **56**, 481 (1984).

²⁷G. M. Minkov, O. E. Rut, A. V. Germanenko, A. A. Sherstobitov, V. I. Shashkin, O. I. Khrykin, and V. M. Daniltsev, *Phys. Rev. B* **64**, 235327 (2001).

²⁸Y. S. Gui, C. M. Hu, Z. H. Chen, G. Z. Zheng, S. L. Guo, J. H. Chu, J. X. Chen, and A. Z. Li, *Phys. Rev. B* **61**, 7237 (2000).

²⁹T. Koga, J. Nitta, T. Akazaki, and H. Takayanagi, *Phys. Rev. Lett.* **89**, 046801 (2002).

- ³⁰K. S. Cho, C.-T. Liang, Y. F. Chen, and J. C. Fan, *Semicond. Sci. Technol.* **22**, 870 (2007).
- ³¹C. Schierholz, T. Matsuyama, U. Merkt, and G. Meier, *Phys. Rev. B* **70**, 233311 (2004).
- ³²S. Iordanski and Y. Levinson, *Phys. Rev. B* **53**, 7308 (1996).
- ³³A. Kabasi and D. Chattopadhyay, *Phys. Rev. B* **43**, 14638 (1991).
- ³⁴I. R. Pagnossin, A. K. Meikap, A. A. Quivy, and G. M. Gusev, *J. Appl. Phys.* **104**, 073723 (2008).